SAND2022-1351J

A Comparison of Radiation-Induced and High-Field Electrically Stress Induced Interface Defects in Si/SiO_2 MOSFETs via Electrically Detected Magnetic Resonance

Fedor V. Sharov, *Student Member, IEEE,* Stephen J. Moxim, *Student Member, IEEE,* Gaddi S. Haase, *Member, IEEE*, David R. Hughart, *Member, IEEE,* Patrick M. Lenahan, *Fellow, IEEE*

***Abstract*— We utilize electrically detected magnetic resonance (EDMR) measurements to compare high-field stressed, and gamma irradiated Si/SiO_2 metal-oxide-silicon (MOS) structures. We utilize spin-dependent recombination (SDR) EDMR detected using the Fitzgerald and Grove dc I-V approach to compare the effects of high-field electrical stressing and gamma irradiation on defect formation at and near the Si/SiO_2 interface. As anticipated, both greatly increase the concentration of P_b centers (silicon dangling bonds at the interface) densities. The irradiation also generated a significant increase in the dc I-V EDMR response of E' centers (oxygen vacancies in the SiO_2 films), whereas the generation of an E' EDMR response in high-field stressing is much weaker than in the gamma irradiation case. These results likely suggest a difference in their physical distribution resulting from radiation damage and high electric field stressing.**

***Index Terms*— Electrically detected magnetic resonance (EDMR), spin-dependent recombination (SDR), radiation damage, high-field stressing, time dependent dielectric breakdown (TDDB).**

I. Introduction

DUE to the near universal presence of the Si/SiO_2 interface in modern integrated circuity, there has been significant interest in quantifying the chemical nature of its performance limiting defects and in how to produce more reliable devices. Magnetic resonance can provide insight into the fundamental physical phenomena and may offer technological insights for the development of more reliable devices [1-8]. Significant insight into reliability physics issues has been provided by various electron paramagnetic resonance (EPR) techniques which offer unrivaled ability to identify atomic-scale structure of radiation [8-16] and other reliability phenomena [17-28] in the Si/SiO_2 system. In this study, we compare the atomic scale defect generation phenomenon in radiation damage and high-field oxide stressing.

Manuscript received October 30th, 2021; revised December 6th, 2021; received XXXXX. Data of publication XXXXXXX; date of current version XXXXXXXX. Sandia National Laboratories (SNL) is a multimission laboratory managed and operated by National Technology and Engineering Solutions of Sandia, LLC, a wholly owned subsidiary of Honeywell International Inc., for the U.S. Department of Energy's National Nuclear Security Administration under contract DE-NA0003525. This paper describes objective technical results and analysis. Any subjective views or opinions that might be expressed in the paper do not necessarily represent the views of the U.S. Department of Energy or the United States Government.

II. Electrically Detected Magnetic Resonance

In magnetic resonance, one subjects a sample to an oscillating magnetic field of frequency v, and a large magnetic field of magnitude $\boldsymbol{B}$ [29]. In the simplest case, the condition for an otherwise isolated electron spin, the resonance condition is given as:

$$hv = g_e \mu_B \boldsymbol{B}. \quad (1)$$

For this simple case, μ_B is the Bohr magneton, g_e = 2.0023 is the Lande g-factor, and $\boldsymbol{B}$ is the applied magnetic field. In real systems, interactions, primarily spin-orbit coupling and electron-nuclear hyperfine coupling, alter this condition. Including these two effects, a spin Hamiltonian for the system can be written as

$$H = \mu_B \boldsymbol{B} \cdot \boldsymbol{g} \cdot \boldsymbol{S} + \boldsymbol{\Sigma_i A_i} \cdot \boldsymbol{I_i} \cdot \boldsymbol{S}. \quad (2)$$

In this expression, $\boldsymbol{g}$ is an orientation dependent value, typically expressed as a second rank tensor that describes the effects of spin orbit coupling. The product $\boldsymbol{A_i I_i}$ describes electron-nuclear hyperfine interactions, where $\boldsymbol{A_i}$ is a second rank tensor and $\boldsymbol{I_i}$ represents the spin on the $\boldsymbol{i}$th nucleus. Analysis of resonance results in terms in expression (2) frequently allows for the determination of the chemical nature of a given paramagnetic defect.

The conventional magnetic resonance technique EPR, which operates on the detection of absorbed power within the system under study at resonance, is sensitive to about 10^{10} total spins and can identify the atomic-scale nature of defects in bulk samples [30] but it lacks the sensitivity to identify defects within semiconductor devices such as MOSFETs and cannot provide information about the physical location of the defects. However, EPR can be made much more sensitive through the technique called electrically detected magnetic resonance (EDMR). EDMR differs from EPR in its detection scheme: spin-dependent phenomena are monitored via changes in device current or voltage. A block diagram of a high-frequency EDMR

F. V. Sharov, S. J. Moxim, and P. M. Lenahan are with the Department of Engineering Science and Mechanics, Pennsylvania State University, State College, PA 16802 USA (e-mail fvs5123@psu.edu).

G. S. Haase and D. R. Hughart are with Sandia National Laboratories, Albequerque, NM 87123 USA.

spectrometer is shown in Fig. 1. The most commonly utilized EDMR technique involves detection of spin-dependent recombination (SDR) [12-17,23-28]. EDMR sensitivity is about 10^7 times greater than that of conventional EPR [31].

One particularly convenient scheme for MOSFET EDMR is the Fitzgerald and Grove dc I-V gated diode approach [32]. In the dc I-V approach, the source/drain to body diodes are slightly forward biased to inject minority carriers into the channel, while the gate is swept from inversion to accumulation. The body is grounded, and the source/drain to body current is measured as function of gate voltage. A schematic of the dc I-V biasing scheme and a recombination current versus gate voltage characteristic is shown in Fig. 2.

At some gate voltage, an equal number of electrons and holes will be present at the interface, maximizing recombination in interface traps. This results in a peak in the body current. This peak in source/drain to body current is related to interface trap density by the expression:

$$\Delta I_{DCIV} = \frac{1}{2} q n_i \sigma v_{th} D_{it} A q |V_f| \exp\left(\frac{q|V_f|}{2k_B T}\right). \quad (3)$$

Here, D_{it} is the density of traps per unit area in the vicinity of the middle of the silicon band gap at the Si/SiO_2, A is the gate area, n_i is the intrinsic carrier concentration, σ is the geometric mean of the capture cross section for holes and electrons, and v_{th} is the thermal velocity. The value V_f is the forward bias of the source and drain to body junction, and q, k_B, and T correspond to the elementary charge, Boltzmann's constant, and temperature, respectively. As discussed by Grove et al. [32], the technique measures interface traps within about $\pm\frac{1}{2}q|V_f|$ of mid-gap.

The EDMR dc I-V approach has been very useful in analyzing radiation damage [12-17]. However, there has been far less research utilizing EDMR in studies of high-field stressed MOS devices [20-22]. While the electrical characteristics of leakage currents due to high-field stress [33-36] and irradiation have been extensively explored, the differing roles of specific defects within SiO_2 in breakdown are not well understood.

III. RELEVANT DEFECTS

Although several paramagnetic defects have been detected in (100) Si/SiO_2 structures via magnetic resonance, the most important defects in (100) Si/SiO_2 devices are the oxide E' and interface P_{b0} and P_{b1} centers. The E' center is a paramagnetic oxide trap that involves a dangling bond on a central silicon atom that is back bonded to three oxygens [2-6, 8-11]. In irradiated MOS devices they are generally holes in oxygen vacancies. P_b centers are interface dangling bonds: trivalent silicons at the Si/SiO_2 interface back bonded to three silicon atoms [1,2,7]. In (100) Si/SiO_2 structures, there can be two similar but geometrically slightly different defect centers: the P_{b0} and the P_{b1} [1,2]. The (100) P_{b0} center is chemically identical to the (111) P_b center. The P_{b1} center similar to the P_{b0}, but with a different structure to its back bonding; this difference leads to its lack of axial symmetry, and a somewhat different g-tensor.

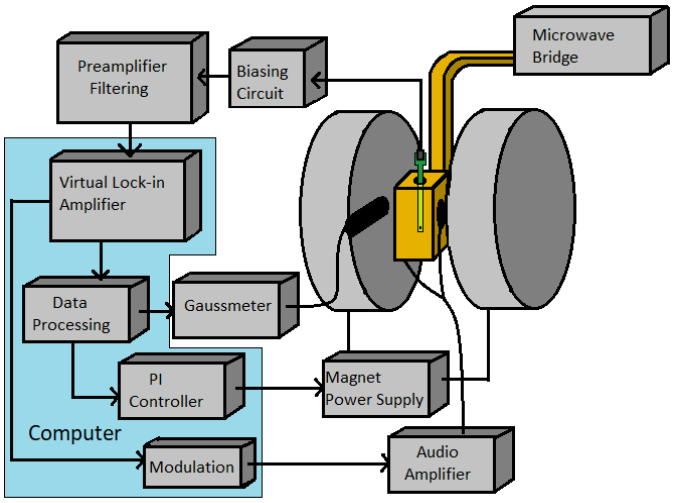

Fig. 1. A block diagram for a high-frequency EDMR spectrometer.

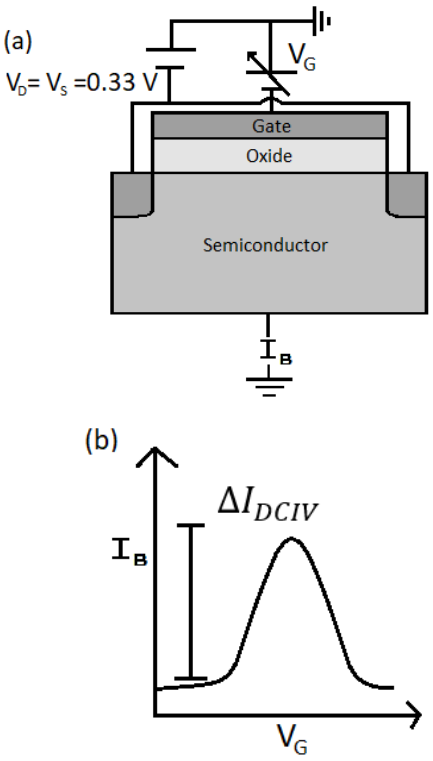

Fig. 2. (a) An example of the dc I-V biasing scheme in a generic MOS device. An example of the measurement output is shown in (b) in which the change in body current is measured as a function of gate voltage.

Previous studies have compared the EPR spectra of irradiated and high-field stressed Si/SiO_2, however, these studies were done on (111) Si/SiO_2 films [18,19]. Warren et al. found that both gamma irradiation and high-field stressing results in the generation of E' centers in (111) Si/SiO_2 "thick" (t>110 nm) films but was unable to resolve an EPR spectrum in "thin" films ($t = 23$ nm) [19]. After the high-field stress, Warren et al. found that the application of ultraviolet (UV) light led to the annihilation of the E' center spectrum, and subsequent

formation of (111) P_b centers [18]. Warren argues that this UV illumination results in photo-injection of negative charge carriers and the return of an electron to the positively charged E' center, rending the defect diamagnetic and neutral. This changes the band bending at the interface leading to an increase in the percentage of P_b centers which are neutral and paramagnetic, and thus EPR detectable.

In a later study, Jupina et al. used the increased sensitivity of EDMR via dc I-V to study the interface of MOSFETs which were subjected to gamma radiation [12]. Jupina et al. identified two near-interface defects generated due to irradiation in their transistors: the P_{b0} and E' center. However, the comparative effects of high-field stressing and radiation damage were never addressed.

IV. Experimental Set-Up

The devices used in this study were identical custom-built 1.89×10^{-5} cm^2 Si/SiO_2 n-type MOSFET structures with 7.5 nm thick oxides. The MOS structures consisted of 126 devices, with 15 by 1 µm channel dimensions. The dc I-V measurements were made using a Hewlett Packard 4155A semiconductor parameter analyzer. All dc I-V measurements were made with a source and drain bias of -0.33 V while sweeping the gate voltage between -2.0 and +2.0 V. This source and drain to body bias was kept constant throughout our studies, and was selected due to the high signal-to-noise of the EDMR measurements at this bias. The high-field dc I-V EDMR measurements were made using a commercial (Bruker Biospin) X-band EPR spectrometer with EDMR detection facilitated by a Stanford Research Systems SR570 low-noise current to voltage preamplifier, using a virtual lock-in detection scheme. The source and drain of these devices were biased at -0.33 V and the gate was set to the bias corresponding to the peak in body current.

Two sets of devices were gamma irradiated to 5 Mrad (Si) and 15 Mrad (Si). The irradiation was performed using a ^{60}Co source under a positive gate bias of +1.5 V at a dose rate of a couple hundred kRad (Si)/hour. Electrical stressing was done by applying a $\pm$ 9.0 V bias to the gates of the MOS devices for 20 minutes with the body, drain, and source grounded. These stressing conditions were selected based on a constant-voltage breakdown study of these MOS devices, corresponding to a near-end of life device. Leakage current versus stress time plots were taken during the high-field stress treatments, with leakage current decreasing over time, as is consistent with the literature [33-36].

Measurements took place within a few days of irradiation as well as high-field stressing, due to the relatively long acquisition times involved in signal averaging of EDMR measurements. Signal averaging provides higher signal to noise for the magnetic resonance spectra: the improvement scales with the square root of acquisition time. Further information about the possible effects of the post-irradiation time evolution of defect sites is presented in the discussion section. Additionally, low-temperature EDMR measurements were performed on the set of high-field stressed devices on the same spectrometer. Low-temperature measurements are used in magnetic resonance literature to enhance sensitivities to certain defects.

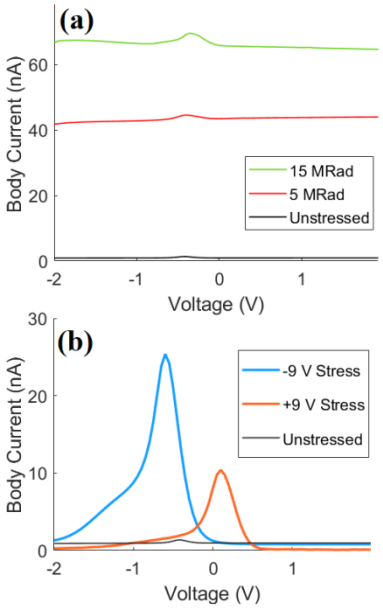

Fig. 3. Measurements of dc I-V on Si/SiO_2 MOS devices for pre- and post- (a) irradiated and (b) high-field stressed devices. The drain and source voltages were set as -0.33 V. Note that irradiation dose significantly increased the baseline current, but the high-field stressing resulted in significantly larger ΔI_{DCIV} currents.

Interface trap densities measured using dc I-V

	Unstressed	- 9 V	+ 9 V	5 Mrad	15 Mrad
Mid-gap D_{it} (10^{11} cm^{-2} eV)	0.12	11	4.5	0.60	1.6

Interface trap densities near the middle of the band gap for the unstressed, high-field electrically stressed ($\pm$ 9 V), and gamma irradiated (5 Mrad (Si) and 15 Mrad (Si)) Si/SiO_2 MOS devices.

V. Results

A. Electrical dc I-V Characteristics

The dc I-V characteristic curves of the unstressed, high-field stressed, and gamma irradiated MOS devices are shown in Fig. 3, while the interface trap densities for defects near the middle of the Si/SiO_2 bandgap extracted from the dc I-V curves are shown in Table 1. Both irradiations and high-field stressing treatments generated much higher dc I-V peaks than are present in the unstressed devices. The unstressed devices have dc I-V peak currents of about 0.4 nA: barely visible above the noise floor. The devices subjected to -9.0 V of gate bias stress for 20 minutes resulted in the highest dc I-V peak current: around 25 nA. The device stressed with +9.0 V at the gate for 20 minutes had a dc I-V peak current of about 10 nA. The two heavily irradiated devices both had much smaller dc I-V peak currents, but significantly higher substrate currents in accumulation and inversion at the same source/drain bias.

B. High-field Stressing EDMR

In the case of MOS devices, EDMR spectra are most readily interpreted by their g-values, as a function of the sample's orientation in the magnetic field. The value of the center field will be proportional to the microwave frequency used in the

measurement based on (1). The g-values as a function of sample orientation in the magnetic field for paramagnetic defects in Si/SiO_2 are very well characterized in literature [1-7]. In a complicated system with two or more EDMR signals with similar enough g-values, there may be overlap of the signals that makes it difficult to separate out the responses. In these cases, it is often helpful to analyze the second derivative of the spectrum, because the second derivative will produce a sharper maximum at the signal's zero-crossing g. Simulations can also help in deconvoluting a multiple defect system.

The high-frequency EDMR comparisons of the unstressed and the electrically stressed devices and their derivatives are shown in Fig. 4 (a) and (b), respectively. In all EDMR measurements, devices were oriented with the magnetic field perpendicular to the (100) interface plane at room temperature. The microwave frequencies used in these measurements were 9.4026 GHz for the positively stressed device and 9.3994 GHz for the negatively stressed device. Otherwise, all EDMR measurements were taken with identical EDMR spectrometer settings with a modulation amplitude of 0.2 mT in order to avoid broadening the linewidths of the narrowest EDMR features.

EDMR measurements on the unstressed devices were below our detection limits. The two defects identified in the EDMR measurements of the high-field stressed devices in Fig. 4 (a) are the interface silicon dangling bond defects known as P_b centers [1,2,7]. With the magnetic field oriented perpendicular to the (100) interface plane, two P_b center signals may appear, one corresponding to the P_{b0} (g = 2.0065) and the other to the P_{b1} (g = 2.0032) [2,7]. It can be difficult to interpret the zero-crossing g-values of these two overlapping defects in the ordinary EDMR spectra. The second derivatives in Fig. 4 (b), which show "peaks" at the locations of the zero-crossing g-values, more clearly illustrate both the existence and location of the two P_b center variants. The EDMR spectra in Fig. 4 (a) and (b) were taken with identical EDMR spectrometer settings with a modulation amplitude of 0.2 mT.

Further confirmation of the existence of both the P_{b0} and P_{b1} centers in the electrically stressed samples can be seen in the wide scan "hyperfine" measurements in Fig. 5. These measurements were taken with slightly different spectrometer settings than those of Fig. 4 to render the side peaks due to the hyperfine interactions more readily visible (modulation amplitude of 0.6 mT). Since about 4.7% of silicon nuclei are magnetic with magnetic moments with nuclei spin ½, additional weak side peaks form, each of intensity 2.35%; these side peaks can be visible in high signal to noise EDMR traces. The P_{b0} and P_{b1} hyperfine peaks are clearly separated by 9.8 mT and 14.5 mT, respectively.

C. Radiation-Damage EDMR

The high-frequency EDMR comparisons of the unstressed devices and the irradiated devices and their derivatives are shown in Fig. 6 (a) and (b). In all three of these EDMR measurements, devices were oriented with the magnetic field perpendicular to the (100) interface plane with microwave frequencies of 9.3996 GHz for the 5 Mrad (Si) irradiated devices, and 9.6214 GHz for the 15 Mrad (Si) irradiated device. These frequencies were scaled to a consistent frequency in the

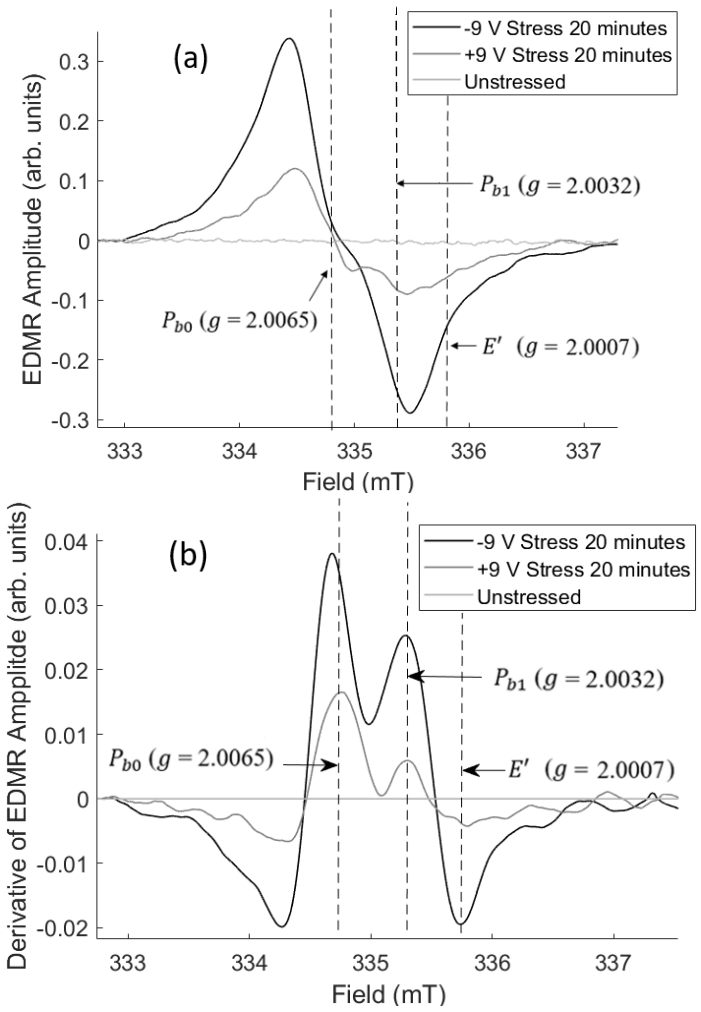

Fig. 4. (a) High-field EDMR detection of dc I-V current in high-field electrically stressed Si/SiO_2 MOS devices and (b) its derivative. The magnetic field is perpendicular to the (100) interface plane in these measurements. The dashed lines correspond to the locations of the P_{b0}, P_{b1}, and E' centers. The only two defects that are visible are the P_{b0} and the P_{b1} center.

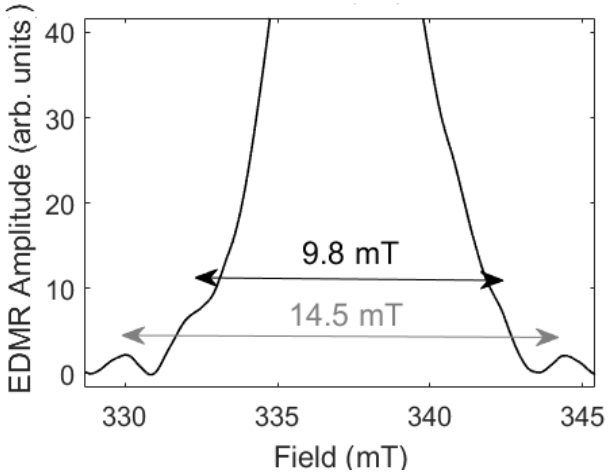

Fig. 5. Hyperfine measurement of the high-field stressed Si/SiO_2 MOS devices from the EDMR absorption spectrum. The spectrum contains two pairs of peaks, corresponding to both the barely visible P_{b0} (9.8 mT) and the more prominent P_{b1} (14.5 mT) hyperfine splitting.

comparative plot. Again, all EDMR measurements were taken with identical EDMR spectrometer settings with a modulation amplitude of 0.2 mT in order to avoid broadening the linewidths of the narrowest EDMR features.

The defects observed in the irradiated devices shown in Fig. 6 include P_{b0} centers, but we are unable to observe clear evidence of a significant P_{b1} center contribution. This result is consistent with earlier studies by Jupina et al. which have also reported a prevalence of P_{b0} in irradiated devices in much thicker oxides [12]. The irradiation did, however, produce a room-temperature detectable E' center response. These defects involve a dangling bond on the central silicon atom back bonded to three oxygens. They are generally holes trapped in oxygen vacancies in gamma irradiated gate oxides. The "zero-crossing" g-value corresponding to the E' center is about 2.0007 [4-6]. For the 5 Mrad (Si) device, the two zero-crossing g-values were g =2.0008 and g = 2.0064. For the 15 Mrad (Si) device, the zero-crossing g-values were g = 2.0007 and g = 2.0068.

Further evidence for the lack of a significant P_{b1} center generation can also be seen in the wide hyperfine spectrum of the 15 Mrad (Si) gamma irradiated device in Fig. 7. Again, these "wide" scans were done at slightly different spectrometer settings than Fig. 6 to render the side peaks due to hyperfine interactions more readily visible (modulation amplitude of 0.6 mT). While the 9.8 mT hyperfine peaks, corresponding to the P_{b0} center, are clearly present in the integrated spectra, it is not clear that there is any formation of 14.5 mT peaks associated with the P_{b1} centers. Additionally, there is some asymmetry in spectra that could in part be due to a small concentration of P_{b1} centers forming.

D. Theoretical Simulations via EasySpin

For the simulations in Fig. 8, we used the EasySpin EPR spectrum fitting tool [37] to fit the EDMR spectra for the positively stressed, negatively stressed, and gamma irradiated device. These spectra were simulated by using literature EPR parameters for the P_{b0}, P_{b1}, and the E' center g-tensors and linewidths. The individual intensities of the P_{b0}, P_{b1}, and the E' center lines were weighted at different percentages of the total EDMR spectra. The g-values used for these defects in the simulations were g=2.0062 for the P_{b0} center, g=2.0030 for the P_{b1} center, and g= [2.0002 2.00018] for the E' center.

Fig. 8 (a) shows the modeling for the negatively stressed device, with a 73% weighting in P_{b0} and 27% weighting in P_{b1}. Fig. 8 (b) shows the modeling for the positively stressed device, with a 87% weighting in P_{b0} and 13% weighting in P_{b1}. The ratio of P_{b0} to P_{b1} changes significantly between the negative and positive high-field stress: a change from about 3:1 to 6:1.

The gamma irradiated device was a little trickier to model. While the gamma irradiated EDMR data shows a clear response associated with the P_{b0} center, the ratio of P_{b0} to P_{b1} centers isn't entirely clear. The EDMR derivative data for the gamma irradiated device in Fig. 6 (b) does not show a significant contribution of P_{b1}, but the asymmetry of the signal in Fig. 6 (a) does suggest the presence of a weak P_{b1} contribution. This suggestion is probably accurate, as the concentration of P_{b1} defects seen in EDMR is known to increase with time after

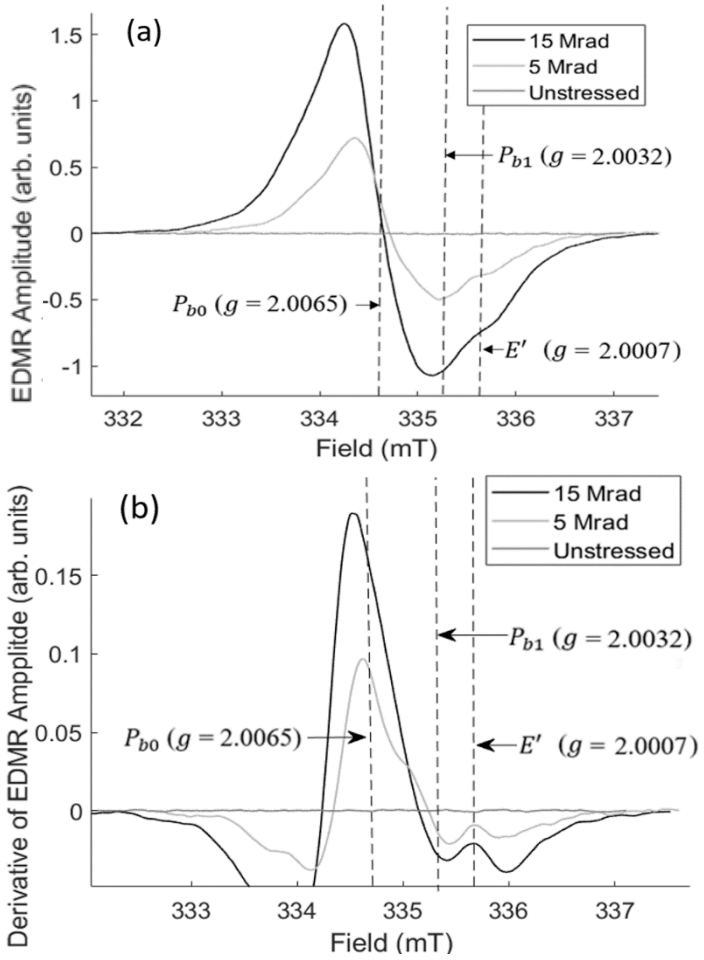

Fig. 6. (a) High-field EDMR detection of dc I-V current in gamma irradiated Si/SiO_2 MOS devices and (b) its derivative. The magnetic field is perpendicular to the (100) interface plane in these measurements. The dashed lines correspond to the locations of the P_{b0}, P_{b1}, and E' centers. The only two defects that are visible are the P_{b0} and the E' center.

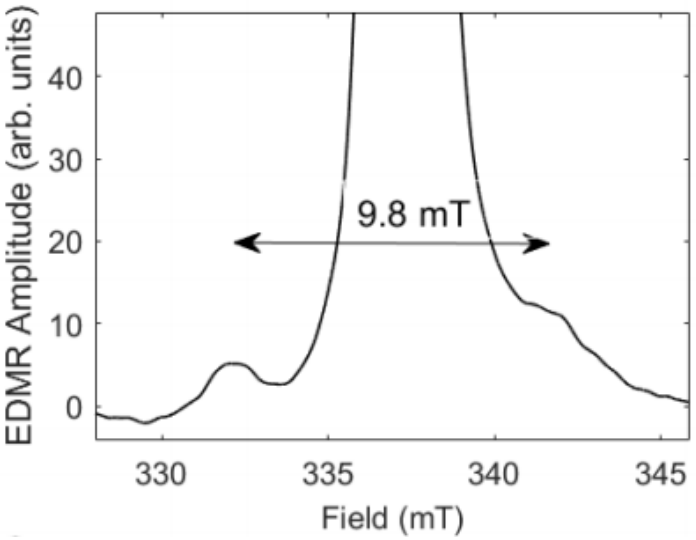

Fig. 7. Hyperfine measurement of the 15 Mrad (Si) gamma irradiated Si/SiO_2 MOS devices from the EDMR absorption spectrum. The spectrum contains only one pair of peaks, corresponding to the clearly visible P_{b0} (9.8 mT).

irradiation [15], and the experiments were done within 72 hours of irradiation. However, even when adding a small amount of P_{b1} as to not distort the lineshape of the EDMR signal, the simulations in Fig. 8 (c) indicate that the irradiation produced the smallest amount of P_{b1} centers relative to the overall signal compared to both high-field stressing treatments for the given time after irradiation.

E. Low-Temperature (200 K) EDMR Measurements

In order to investigate whether there was an E' center response in the high-field stressed MOSFETs, we also performed low-temperature (200 K) EDMR measurements on the high-field stressed oxides. The EDMR spectra for this measurement are shown in Fig. 9, which shows an additional EDMR response corresponding to the E' center (g=2.000) [6,7]. The appearance of this signal at this temperature is most likely due to the lengthening of the spin lattice relaxation times of E' center due to the lower temperatures.

VI. Discussion

The EDMR results shown in Figs. 4-9 clearly show strong generation of P_{b0} centers in both gamma irradiation and high-field stressing. Additionally, the EDMR spectra shows a generation of E' centers due to both damage mechanisms; however, the generation of E' centers in the high-field stressed oxides are beneath the detection limits of dc I-V EDMR at room temperature. The high-field stressing results are not all that surprising from a qualitative point of view. Recently, Hori et al. [21] reported on EDMR measurements of high-field stressed MOS oxides and reported observations of P_{b0} centers and E' centers. The did not, however, observe clear evidence of high-field stressed P_{b1} centers and they also reported a stronger E' response relative to the P_{b0} response than we observe. Also, much earlier conventional EPR results by Warren et al. [18,19] on high-field stressed oxides on (111) Si/SiO_2 structures reported generation of both E' centers and the P_b variant that is observed on (111) Si/SiO_2 interfaces. Warren et al. also reported roughly comparable P_{b0} and E' amplitudes.

Firstly, as EPR studies and purely electrical measurement studies have shown, there is substantial generation of Si/SiO_2 interface traps, revealed by EPR/EDMR measurements to be P_b centers. Secondly, the generation of E' EDMR spectra with high-field stressing is much weaker than that of the P_b centers and also relatively weaker compared to the P_b response observed in conventional EPR. The dc I-V EDMR response is inevitably very sensitive to near interface traps, but far less sensitive to defects further in the oxides. This is because of the physical nature of the EDMR response, which involves electron-hole pair recombination. Our results combined with the results of the earlier studies strongly suggest that the E' centers in high-field stressing are far more broadly [33] distributed in the oxides than is the case in radiation damage [4]. It should be noted that the formation of a strong P_{b1} center response is qualitatively similar to what takes place in negative bias temperature instability (NBTI) [23-26].

The dc I-V EDMR results in Figs. 6 and 7 show a clear generation of P_{b0} and E' centers with increasing irradiation dosage. This observation is consistent with previous dc I-V

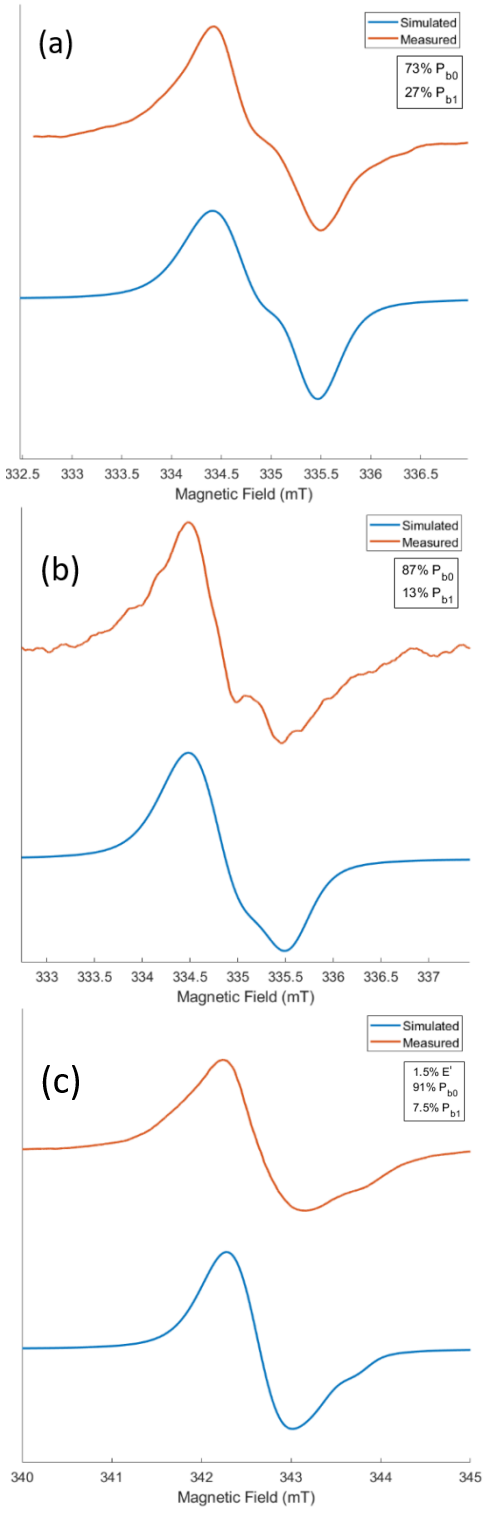

Fig. 8. EasySpin [40] simulations vs. room-temperature EDMR measurements for the (a) – 9 V stress, (b) + 9 V stress, and (c) 15 Mrad (Si) gamma irradiation treatments. The (a) negatively high-field stressed device has the largest contribution from the P_{b1} defect. The positively stressed (b) has around a factor of 2 lower P_{b1} concentration. The gamma irradiated device (c) was the only one that had a noticeable E' generation, measured at around 1.5% of the total spectra. While there is no clear P_{b1} signal, we simulated the largest amount of it without affecting the signal in order to somewhat match the asymmetry. It is important to note that the calculated value for the E' concentration does not reflect the relative concentration of E' centers. These EDMR measurements are only weakly sensitive to defects within the oxides, with sensitivity which drops as a function

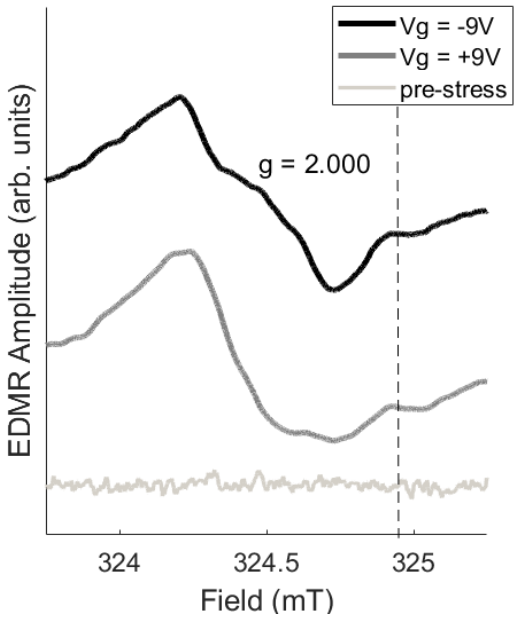

Fig. 9. Low-temperature (200 K) dc I-V EDMR spectra of high-field stressed Si/SiO_2 MOS devices. In this case, both the P_{b0}, P_{b1}, and E' (g=2.000) are clearly visible.

EDMR studies by Jupina et al [12]. However, the ratio of E' centers to P_{b0} centers is significantly different, likely due to a difference in oxide quality and thickness. Additionally, there is no clear evidence of P_{b1} center generation in the irradiated EDMR spectra; the hyperfine EDMR in Fig. 7 shows clear evidence of peaks associated with the P_{b0} center, but not the P_{b1} center. The absence of a significant P_{b1} center formation is also similar to the interface breakdown that occurs in hot carrier stressing [27,28]. The only evidence of a potential P_{b1} center contribution stems from the asymmetry in the spectra, which would indicate there is some contribution from P_{b1} centers to the overall line shape of the EDMR spectra, albeit significantly less than in the case of high-field stressing. We address this possibility using theoretical EPR simulations shown in Fig. 8.

It should be noted, however, that the observation of these defect concentrations is not entirely quantitatively accurate. The distribution of E' centers in the oxide will strongly alter their concentration in the EDMR response; i.e, the closer the E' centers are to the interface, the stronger the response. Furthermore, annealing effects due to exposure of temperature and bias have been shown to significantly change density of trapped holes and interface traps [13-15]. The unavoidable time between irradiation and EDMR measurement signal averaging may allow for modest annealing of traps. Previous EPR studies have shown that there is a significant evolution of defect traps as a function of time and bias in Si/SiO_2, primarily shortly after irradiation [14]. Likewise, studies have shown that there is a significant change in the ratios of P_{b0}, P_{b1}, and E' centers over longer periods of time in gamma irradiated Si/SiO_2 MOSFETs [15]. However, the large differences in the EDMR spectra between radiation damage and high-field stressing likely indicates that there is a difference in the defect buildup between these two damage mechanisms. The E' center plays a significant role in the formation of P_{b0} and P_{b1} [8-11, 14-15] defects in radiation damage; it is possible that the complex nature of carrier injection into the oxide during high-field stressing could additionally be acting as the mechanism contributing to the disparities between the EDMR spectra.

VII. Conclusions

In conclusion, our room-temperature comparison of the atomic-scale mechanisms of high-field electrical stressing and gamma irradiation of defects at and near the Si/SiO_2 interface of identical devices show that there are significant atomic scale similarities as well as differences between the two damage mechanisms. As has been reported previously, irradiation does not produce a strong P_{b1} response but does produce a strong E' center response. Conversely, high-field electrical stressing resulted in a strong P_{b1} center EDMR amplitude, but a considerably weaker E' response. This weak response does not prove that E' centers are irrelevant in the high-field stressed devices; a modest difference in the physical locations of these centers could render them nearly invisible in this measurement which is primarily sensitive to interface defects very close to the interface. Our results most likely indicate that there is a significant difference in the distribution of generated E' oxide states, as well as a preferred distribution of generated P_{b0} and P_{b1} silicon dangling bond defects between the two damage mechanisms.

Acknowledgment

Sandia National Laboratories (SNL) is a multimission laboratory managed and operated by National Technology and Engineering Solutions of Sandia, LLC, a wholly owned subsidiary of Honeywell International Inc., for the U.S. Department of Energy's National Nuclear Security Administration under contract DE-NA0003525. This paper describes objective technical results and analysis. Any subjective views or opinions that might be expressed in the paper do not necessarily represent the views of the U.S. Department of Energy or the United States Government.

The devices were irradiated at the Penn State Radiation Science and Engineering Center, which houses a nuclear research reactor for neutron irradiations as well as separate gamma-ray irradiation facilities and laboratories.

References

[1] Y. Nishi, T. Tanaka, and A. Ohwada, "Study of Silicon-Silicon Dioxide Structure by Electron Spin Resonance II," *Jpn. J. Appl. Phys*., vol. 11, no. 1, pp. 85-91, Jan. 1972.

[2] E. H. Poindexter, P. J. Caplan, B. E. Deal, and R. R. Razouk, "Interface states and electron spin resonance centers in thermally oxidized (111) and (100) silicon wafers," *J. Appl. Phys.,* vol. 52, no. 2, pp. 879-884, Feb. 1981.

[3] P. M. Lenahan and P. V. Dressendorfer, "Hole traps and trivalent silicon centers in metal/oxide/silicon devices," *J. Appl. Phys.,* vol. 55, no. 2, pp. 3495-3499, May 1984.

[4] Y. Y. Kim and P. M. Lenahan, "Electron-spin-resonance study of radiation-induced paramagnetic defects in oxides grown on (100) silicon substrates," *J. Appl. Phys*., vol. 64, no. 7, pp. 3551–3557, Oct. 1988.

[5] F. J. Feigl, W. B. Fowler, and K. L. Yip, "Oxygen Vacancy model for the E_1' center in SiO_2," *Solid State Commun.,* vol. 14, no. 3, pp. 225-229, Feb. 1974.

[6] L. Lipkin, L. Rowan, A. Reisman, and C. K. Williams, "Correlation of Fixed Positive Charge and E'$_\gamma$ Centers as Measured via Electron Injection and Electron Paramagnetic Resonance Techniques," *J. Electrochem. Soc*., vol. 138, no. 7, pp. 2050-2052, Jul. 1991.

[7] A. Stesmans, B. Nouwen, and V. V. Afanas'ev, "P_{b1} interface defect in thermal (100) Si/SiO_2: ^{29}Si hyperfine interaction," *Phys. Rev. B*, vol. 58, no. 23, pp. 15801-15809, Dec. 1998.

[8] P. M. Lenahan, J. J. Mele, J. F. Conley, R. K. Lowry, and D. Woodbury, "Predicting Radiation Response from Process Parameters: Verification of Physically Based Predictive Model," *IEEE Trans. Nucl. Sci.,* vol. 46, no. 6, pp. 1534-1543, Dec. 1999.

[9] P. M. Lenahan and J. F. Conley, "A comprehensive physically based predictive model for radiation damage in MOS systems," *IEEE Trans. Nucl. Sci.,* vol. 45, no. 6, pp. 2413-2423, Dec. 1998.

[10] P. M. Lenahan, J. F. Conley, and B. D. Wallace, "A model of hole trapping in SiO_2 films in silicon," *J. Appl. Phys.*, vol. 81, no. 10, pp. 6822-6824, May 1997.

[11] P. M. Lenahan and J. F. Conley, "A physically based predictive model of Si/SiO_2 interface trap generation resulting from the presence of holes in the SiO_2," *Appl. Phys. Lett.*, vol. 71, no. 21, pp. 3126-3128, Nov. 1997.

[12] P. M. Lenahan and M. A. Jupina, "Spin dependent recombination at the silicon/silicon dioxide interface," *Colloids Surf.*, vol. 45, pp. 191-211, 1990.

[13] T. R. Oldham and F. B. McLean, "Total Ionizing Dose Effects in MOS Oxides and Devices," *IEEE Trans. Nucl. Sci.,* vol. 50, no. 3, pp. 483-499, Jun. 2003.

[14] J. F. Conley, P. M. Lenahan, A. J. Lelis, and T. R. Oldham, "Electron Spin Resonance Evidence that E'_γ Centers Can Behave as Switching Oxide Traps," *IEEE Trans. Nucl. Sci*., vol. 42, no. 6, pp. 1744-1749, Dec. 1995.

[15] P. M. Lenahan, T. D Mishima, J. Jumper, T. N. Fogarty, and R. T. Wilkins, "Direct Experimental Evidence for Atomic Scale Structural Changes Involved in the Interface-Trap Transformation Process," *IEEE Trans. Nucl. Sci*., vol. 48, no. 6, pp. 2131-2135, Dec. 2001.

[16] W. Akhtar, H. Morishita, L. S Vlasenko, D.S. Poloskin, and K. M. Itoh, "Electrically detected magnetic resonance of phosphorous due to spin dependent recombination with triplet centers in γ-irradiated silicon," *Phys. Rev. B Condens*. *Matter*, vol. 404, no. 23-24, pp. 4583-4583, Dec. 2009.

[17] K. J. Myers, R. J. Waskiewicz, P. M. Lenahan, and C. D. Young, "A Multifield and Frequency Electrically Detected Magnetic Resonance Study of Atomic-Scale Defects in Gamma Irradiated Modern MOS Integrated Circuitry," *IEEE Trans. Nucl. Sci*., vol. 66, no. 1, pp. 405-412, Jan. 2019.

[18] W. L. Warren and P. M. Lenahan, "Electron spin resonance study of high field stressing in metal-oxide-silicon device oxides," *Appl. Phys. Lett.*, vol. 49, no. 19, pp. 1296-1298, Nov. 1986.

[19] W. L. Warren and P. M. Lenahan, "A Comparison of Positive Charge Generation in High Field Stressing and Ionizing Radiation on MOS Structures," *IEEE Trans. Nucl. Sci.*, vol. 34, no. 6, pp. 1355-1358, Dec. 1987.

[20] J. H. Stathis, "Electrically detected magnetic resonance study of stress-induced leakage current in thin SiO_2," *Appl. Phys. Lett.,* vol. 68, no. 12, pp. 1669-1671, Mar. 1996.

[21] M. Hori and Y. Ono, "Charge Pumping Under Spin Resonance in Si (100) Metal-Oxide-Semiconductor Transistors," *Phys. Rev. Appl.*, vol. 11, no. 6, Jun. 2019, Art. no. 064064.

[22] S. J. Moxim, J. P. Ashton, P. M. Lenahan, M. E. Flatté, N. J. Harmon, and S. W. King, "Observation of Radiation-Induced Leakage Current Defects in MOS Oxides with Multifrequency Electrically Detected Magnetic Resonance and Near-Zero-Field Magnetoresistance," *IEEE Trans. Nucl. Sci.*, vol. 67, no. 1, pp. 228-233, Jan. 2020.

[23] J. T. Ryan, P. M. Lenahan, T. Grasser, and H. Enichlmair, "Observations of negative bias temperature instability defect generation via on the fly electron spin resonance," *Appl. Phys. Lett*., vol. 96, no. 2, Jun. 2010, Art. no. 223509.

[24] J. P. Campbell, P. M. Lenahan, C. J. Cochrane, A. T. Krishnan, and S. Krishnan, "Atomic-scale defects involved in the negative-bias temperature instability," *IEEE Trans. Device Mater. Reliab*., vol. 7, no. 4, pp. 540-557, Dec. 2007.

[25] J. P. Campbell, P. M. Lenahan, A. T. Krishnan, and S. Krishnan, "Identification of atomic-scale defect structure involved in the negative bias temperature instability in plasma-nitrided devices," *Appl. Phys. Lett*., vol. 91, no. 13, Sep. 2007, Art. no. 133507.

[26] T. Aichinger, P. M. Lenahan, and D. Peters, "Interface Defects and Negative Bias Temperature Instabilities in 4H-SiC PMOSFETs – A Combined DCIV/SDR Study," *Mater. Sci. Forum*., vols. 740-742, pp. 529-532, Jan. 2013.

[27] J. W. Gabrys, P. M. Lenahan, and W. Weber, "High resolution spin dependent recombination study of hot carrier damage in short channel MOSFETs: ^{29}Si hyperfine spectra," *Microelectron. Eng*., vol. 22, no. 1-4, pp. 273-276, Aug. 1993.

[28] D. J. DiMaria and J. H. Stathis, "Anode hole injection, defect generation, and breakdown in ultrathin silicon dioxide films", *J. Appl. Phys.,* vol. 89, no. 9, pp. 5015-5024, May 2001.

[29] J. A. Weil and J. R. Bolton, *Electron Paramagnetic Resonance: Elementary theory and practical applications*, Hoboken, New Jersey: Wiley-Interscience, 2007, pp. 1-39.

[30] G. R. Eaton, S. S. Eaton, and K. Ohno, *EPR Imaging and in vivo EPR: Sensitivity in EPR imaging*, Boca Raton, Florida: CRC Press, 2018, pp. 162-166.

[31] G. Kawachi, C. F. O. Grae, M. S. Brandt, M. Stutzmann, and M. J. Powell, "Spin-dependent transport in amorphous silicon thin-film transistors," *J. Non-Cryst. Solids*., vol. 198-200, no. 2, pp. 1117-1120, May 1996.

[32] D. J. Fitzgerald and A. S. Grove, "Surface recombination in semiconductors," *Surface Sci.*, vol. 9, no. 2, pp. 347–369, 1968.

[33] J. W. McPherson, *Reliability Physics and Engineering: Time-to-Failure Modeling,* New York: Springer, 2013, pp. 37-49.

[34] D. G. Borse, S. J. Vaidya, and A. N. Chandorkar, "Study of and interface trap generation due to high field stressing and its operating temperature dependence in 2.2 nm gate dielectrics," *IEEE Trans. Electron Devices,* vol. 49, no. 4, pp. 699-701, Apr. 2002.

[35] R. Moazzami and C. Hu, "Stress-induced current in thin dioxide films," *Int. Tech. Dig. Electron. Dev. Mtg.,* pp. 139-142, Dec. 1992.

[36] A. Padovani, D. Z. Gao, A. L. Shluger, and L. Larcher, "A microscopic mechanism of dielectric breakdown in SiO_2 films: An insight from multi-scale modeling," *J. Appl. Phys.,* vol. 121, no. 15, Apr. 2017, Art. no. 155101.

[37] S. Stoll and A. Schweiger, "EasySpin, a comprehensive software package for spectral simulation and analysis in EPR", *J. Magn. Res.*, vol. 178, no. 1, pp. 42-55, Jan. 2006.